LBL-21387

Lawrence Berkeley Laboratory

UNIVERSITY OF CALIFORNIA

Accelerator & Fusion Research Division

Presented at the 13th International Conference on High Energy Accelerators, Novosibirsk, USSR, August 7-11, 1986

SIMULATION OF SYNCHROTRON MOTION WITH RF NOISE

B.T. Leemann, E. Forest, and S. Chattopadhyay

August 1986

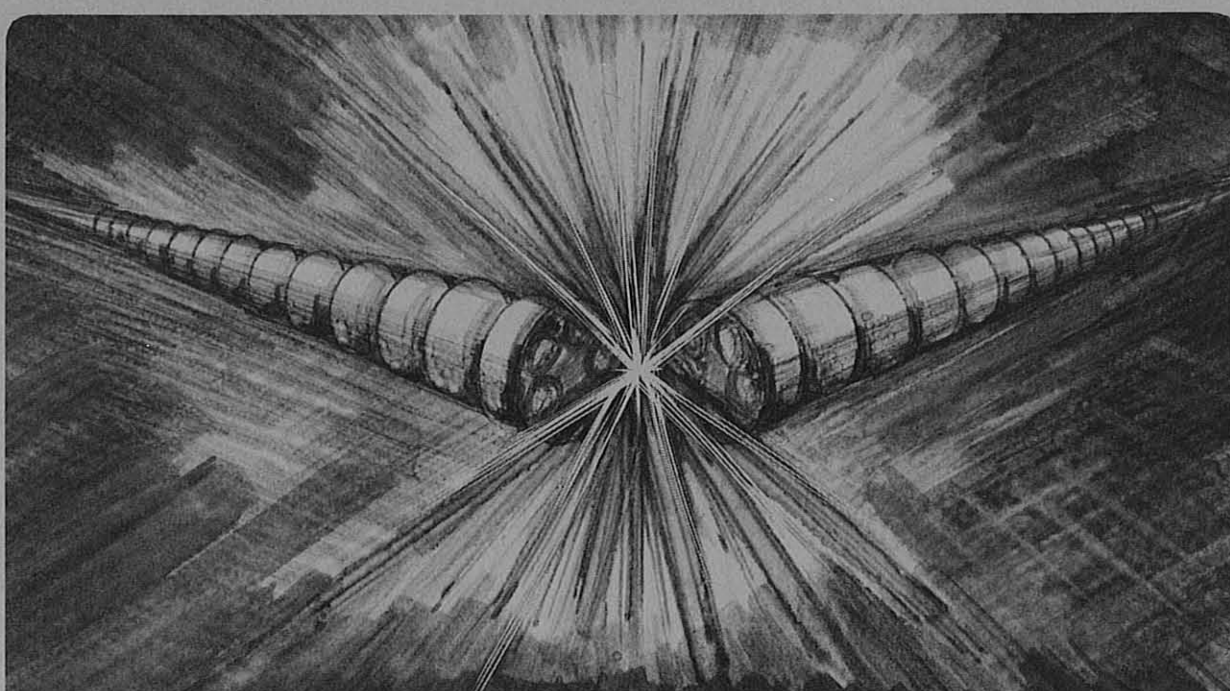

Prepared for the U.S. Department of Energy under Contract DE-AC03-76SF00098

LBL-21387
ESG-19

SIMULATION OF SYNCHROTON MOTION WITH RF NOISE†**

B.T. Leemann, E. Forest, and S. Chattopadhyay

Lawrence Berkeley Laboratory
University of California
Berkeley, CA 94720

August 1986

*Operated by Universities Research Association for the U.S. Department of Energy.
† SSC-Report 80.
**This work was partially supported by the Office of Basic Energy Sciences of the U.S. Department of Energy, under Contract No. DE-AC03-76SF00098.

SIMULATION OF SYNCHROTRON MOTION WITH RF NOISE[†]

B.T. Leemann, E. Forest, and S. Chattopadhyay
SSC Central Design Group,* c/o Lawrence Berkeley Laboratory, Berkeley, California USA 94720

ABSTRACT

We describe the theoretical formulation behind an algorithm for synchrotron phase-space tracking with rf noise and some preliminary simulation results of bunch diffusion under rf noise obtained by actual tracking.

1. Introduction

Amplitude and phase noise in the voltage of a radio-frequency (rf) cavity in a storage ring induces diffusion of particles in a stored bunch in the longitudinal synchrotron phase space, in absence of other damping mechanisms (e.g., synchrotron radiation). Such noise in the low-level rf system severely limited the beam life-time in the initial operation of the SPS at CERN.[1] A stable oscillator (VCO) with a very low noise figure and a phase feedback loop with a carefully chosen loop transfer function to reduce the overall noise power at the synchrotron frequency, as seen by the beam, cured the problem at the SPS.[1,2] The study of rf noise and possible cures to reduce the induced bunch diffusion continue to be important for future large storage rings such as the SSC in the USA.

The basic theory of bunch diffusion under rf noise is well developed.[3,4] There has also been a preliminary computer simulation of the effects of rf noise on synchrotron motion by Mizumachi.[5] In this paper we describe a synchrotron phase-space tracking for a beam of particles seeing rf noise that differs from the previous work[5] in three additional aspects: (a) use of an improved longitudinal phase-space invariant derived from the discrete synchrotron map; (b) generation of rf phase noise with temporal autocorrelation taken into account; and (c) inclusion of the effects of rf phase feedback used to reduce the noise power seen by the beam. In the following we describe the theoretical formulation behind the algorithm used to include these features and some preliminary simulation results of actual tracking.

2. Discrete Synchrotron Map and Invariant Without Noise

The turn-by-turn finite difference equation for particle motion in a stationary non-accelerating rf bucket ($\psi_s = 0$ or π) in absence of noise is given by the map[3]

$$\mathcal{M}: \quad \begin{aligned} P_{n+1} - P_n &= -kg(\psi_n) \\ \psi_{n+1} - \psi_n &= P_{n+1} \;, \end{aligned} \tag{1}$$

where

$$P_n = \frac{2\pi h\eta}{p_s}\,\delta p_n \;,\; k = 2\pi h|\eta|\frac{eV}{p_s v_s}. \tag{2}$$

Here p_s and v_s are the momentum and velocity respectively of the reference synchronous particle, $\delta p_n = p_n - p_s$, $\psi_n = \delta\phi_n = \phi_n - \phi_s$ are the momentum and rf phase deviations from the synchronous particle, h, the rf harmonic number; η, the off-energy function; V the peak rf voltage; and e the electric charge of the particles. The function $g(\psi)$ describes the shape of the rf voltage with

$$\begin{aligned} g(\psi + 2\pi) &= g(\psi) \\ g(0) &= 0 \end{aligned} \tag{3}$$

(stationary bucket). Typically $g(\psi) = \sin\psi$, with small amplitude synchrotron oscillations sampling an almost linear rf voltage $g(\psi) \approx \psi$. In both cases $g'(0) = 1$. In general, with higher harmonic cavities one has the Fourier series representation

$$g(\psi) = \sum_{n=1}^{\infty} A_n \sin(n\psi); \; g'(0) = \sum_{n=1}^{\infty} A_n . n \;. \tag{4}$$

With Landau cavities used to increase synchrotron frequency spread by producing a nonlinear bucket, one uses $g'(0) = 0$, while for the purpose of maximal linearization of the bucket in order to reduce rf noise effects, one uses $g'(0) = 1$.

The map $\mathcal{M}$ in Eq. (1) can be decomposed into the following two maps (with barred and unbarred variables corresponding to successive turns)

$$\mathcal{M} = \mathcal{M}_1 . \mathcal{M}_2(k) \tag{5}$$

$$\mathcal{M}_1: \begin{aligned} \bar{\psi} &= \psi + P \\ \bar{P} &= P \end{aligned} \qquad \mathcal{M}_2(k): \begin{aligned} \bar{\psi} &= \psi \\ \bar{P} &= P - kg(\psi) \;. \end{aligned} \tag{6}$$

This is represented in Fig. 1(a). To simplify the mathematics and improve the accuracy of the discrete longitudinal invariant obtained perturbatively later on, it is convenient to rewrite the above map and variables so as to refer always to the center of the cavity, with new variables $\tilde{\psi} = \psi$ and $\tilde{P} = (P+\bar{P})/2$. The new map $\tilde{\mathcal{M}}$ is obtained by a similarity transformation $\tilde{\mathcal{M}} = \mathcal{M}_2(k/2)\mathcal{M}\mathcal{M}_2(-k/2)$ and can be written as

$$\tilde{\mathcal{M}} = \mathcal{M}_2(\tfrac{k}{2}) . \mathcal{M}_1 . \mathcal{M}_2(\tfrac{k}{2}) \;. \tag{7}$$

This is represented in Fig. 1(b). An alternative but equivalent reformulation would be obtained instead by always referring to the center of the arc.

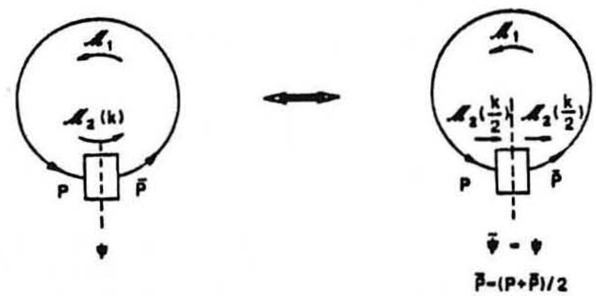

(a) Fig. 1. (b)

For linear rf voltage $g(\psi) = \psi$, it is easy to obtain the quadratic invariant of $\tilde{\mathcal{M}}$. The matrix representation of the linear transformation is

$$\tilde{M} = \begin{bmatrix} 1 - \frac{k}{2} & 1 \\ -\frac{k}{2}(2 - \frac{k}{2}) & 1 - \frac{k}{2} \end{bmatrix} \;. \tag{8}$$

From the usual Courant-Snyder theory, we must have for the Twiss parameters

* Operated by Universities Research Association for the U.S. Department of Energy.
† SSC-Report 80.

$$\sin^2\frac{\mu}{2} = \frac{k}{4}\ ; \quad \mu = \text{tune of } \tilde{\mathcal{M}}. \tag{9}$$

$$\beta = \frac{1}{\sin\mu}, \qquad \gamma = \sin\mu\ ;\ \alpha = 0\ .$$

From Eq. (9), we deduce immediately the quadratic invariant of $\tilde{\mathcal{M}}$

$$I_2 = \tilde{\psi}^2 + (\sin^2\mu)^{-1}\,\tilde{P}^2 = \psi^2 + (P+\tilde{P}/2\sin\mu)^2\ . \tag{10}$$

Clearly this invariant degrades as we go away from the origin in (ψ, P) - space, since the linear approximation $g(\psi) = \psi$ becomes increasingly less accurate. The invariant I_2 is correct to all orders in μ (and hence k) but is only quadratic in (ψ, P). Therefore an expansion in (ψ, P) is not the best choice. Fortunately, the temporal synchrotron tune μ is usually very small ($\mu \sim 10^{-2}$) for large storage rings and provides us with a small parameter that can be exploited in a convergent perturbation scheme. It is thus preferable to keep the nonlinearity in (ψ, P) to all orders and expand in μ. The resulting invariant will be exact in the nonlinearity and expanded up to a certain order of the small parameter μ. (This is exactly opposite to the treatment of nonlinear transverse betatron motion where one stays exact in the betatron tunes ν_x, ν_y, which are large and expands in powers of x, p_x, y and p_y).

A well-defined perturbation approach for the higher order (in μ) invariants is provided by the Lie-algebraic method,[6] where one rewrites $\mathcal{M}_1$ and $\mathcal{M}_2(k/2)$ in terms of Lie operators

$$\mathcal{M}_1 = \exp(:-\frac{\tilde{P}^2}{2}:);\ \ \mathcal{M}_2(\frac{k}{2}) = \exp(:-\frac{k}{2}\Gamma(\psi):)\ . \tag{11}$$

where

$$\Gamma(\psi) = \int_0^{\psi} g(\psi)d\psi = \frac{\psi^2}{2} + \gamma(\psi) \tag{12}$$

$$\text{and } :f:g = [f,\ g] \tag{13}$$

is simply the Poisson bracket operation. $\gamma(\psi)$ is of order 3 and higher in ψ, containing purely the nonlinear part of the rf voltage. The linear parts of the map can be lumped together, thus giving for the full map

$$\tilde{\mathcal{M}} = \exp(:-\frac{k}{2}\gamma(\psi):)\,\tilde{\mathcal{M}}_L \exp(:-\frac{k}{2}\gamma(\psi):)\ , \tag{14}$$

where

$$\tilde{\mathcal{M}}_L = \exp(:-\frac{k}{4}\psi^2:)\exp(:-\frac{\tilde{P}^2}{2}:)\exp(:-\frac{k}{4}\psi^2:)$$

$$= \exp(:-\frac{\mu\sin\mu}{2}\,I_2:)\ . \tag{15}$$

If we can find an H such that $\tilde{\mathcal{M}} = \exp(:H:)$, then H is an invariant. We introduce a "smallness" parameter σ, ultimately to be set to unity, such that

$$\tilde{\mathcal{M}}(\sigma) = \exp(:-\sigma\frac{k}{2}\gamma(\psi):)\,\tilde{\mathcal{M}}_L(\sigma)\ \ \exp(:-\sigma\frac{k}{2}\gamma(\psi):)\ . \tag{16}$$

Assuming the existence of $H(\sigma)$ in the formal power series (in σ) sense as follows

$$H(\sigma) = \sum_{n=1}^{\infty} \sigma^n H_n \tag{17}$$

one can then verify that[6] $H(-\sigma) = -H(\sigma)$, so that only the odd powers n = 1, 3, 5, ... are present in the expansion. One can derive a differential equation for $\tilde{\mathcal{M}}(\sigma)$ with respect to σ and using the properties of Lie operators and their adjoint representation, one obtains[6] a hierarchy of equations for the various H_n. For the standard cavity kick with $\Gamma(\psi) = 1-\cos\psi$, we obtain[6]

$$H_1 = -\frac{\mu}{2\sin\mu}(\psi^2\sin^2\mu + \tilde{P}^2) + 4\sin^2(\frac{\mu}{2})\ (\cos\psi - 1 + \frac{\psi^2}{2}\ ) \tag{18}$$

$$H_3 = \frac{2}{3}\,\frac{\mu\sin^4(\mu/2)}{\sin\mu}(\sin\psi - \psi)^2 +$$

$$\frac{1}{3}\,\frac{\mu^3\sin^2(\mu/2)}{\sin^2\mu}[\sin^2\mu(\psi\sin\psi - \psi^2) - \tilde{P}^2(\cos\psi - 1)]\ . \tag{19}$$

For the general rf voltage given by Eq. (4) with $g'(0) = 0$, one obtains

$$H_1 = -\frac{\tilde{P}^2}{2} + 4\sin^2(\frac{\mu}{2})\left\{\sum_{n=1}^{\infty}\frac{A_n}{n}\ \ [\cos(n\psi)-1] + \frac{\psi^2}{2}\right\} \tag{20}$$

$$H_3 = \frac{2}{3}\sin^4(\frac{\mu}{2})[\sum_{n=1}^{\infty}\ A_n\sin(n\psi)\ - \psi]^2$$

$$-\frac{1}{3}\sin^2(\frac{\mu}{2})\tilde{P}^2\ \sum_{n=1}^{\infty} nA_n[\cos(n\psi)-1]\ . \tag{21}$$

It is easy to check that H_1 in Eq. (18), to order μ^3, can be written as

$$H_1^{DM} = -[\frac{\tilde{P}^2}{2} + \sin^2\mu\ \Gamma(\psi)]\ . \tag{22}$$

This is the same as the "conjectured" Dôme-Miznmachi nonlinear invariant for the discrete synchrotron map.[2,5] We have not only recovered but improved it [Eq. (18)] and obtained higher order invariants as well [Eq. (19), etc.] by a systematic perturbation scheme.

We have tracked particles in the synchrotron phase space, without noise, for many synchrotron oscillations using the map $\mathcal{M}$ given by Eq. (1), and computed the linear quadratic invariant I [Eq. (10)], the nonlinear Dome-Mizumachi invariant[2] H^{DM} [Eq. (22)] and the "improved" nonlinear invariants[1] H_1 and H_3 [Eqs. (18) and (19)] given by our perturbation scheme, for comparison. The relative deviations of H_1^{DM} and H_3 are shown in Figs. 2(a) and (b). The improvement in the invariant is remarkable and obvious from the figure.

3. Discrete Synchrotron Map With Noise

In the bunch frame, any deviation of the designed pure sinusoidal rf field is seen by the particles as a noise in the magnitude and sign of the voltage. In the laboratory frame we can conveniently decompose any deviation of the rf voltage V into a phase error (error in zero-crossing) and an amplitude error as follows

$$V = V_0(1+a)\ \sin(\theta + \nu.\varphi)\ , \tag{23}$$

where a and φ are the relative amplitude and phase noise values, with their randomness determined by the nature of the noise source. Since for the same noise power levels, the phase noise is more destructive than the amplitude noise to the bunch phase-phase,[4,5] we neglect amplitude noise in this article from now on (a=0).

The turn-by-turn finite difference equation for particle motion as given by Eq. (1) are modified in presence of phase noise to

$$P_{n+1} - P_n = -kg(\psi_n)$$
$$\psi_{n+1} - \psi_n = P_{n+1} + \varphi_{n+1} - \varphi_n\ . \tag{24}$$

It is convenient to refer the particle phase relative to a fixed ideal rf waveform (with no noise) at the localized rf cavity (thin lens longitudinally), rather than relative to the jittery rf waveform with noise. In the frame of this absolute clock run by the ideal cavity, the synchrotron map with phase noise may be rewritten as

$$P_{n+1} - P_n = -kg(\psi_n + \varphi_n)$$

$$\psi_{n+1} - \psi_n = P_{n+1} \ . \qquad (25)$$

This is the form we used in the actual tracking.

The phase noise φ_n results from the sampling of a random process every turn. For tracking with Eq. (25), one will have to generate sequences of these random numbers $\{\varphi_n\}$, consistent with the realistic noise characteristics of a driven rf cavity. We thus turn to this issue in the next section.

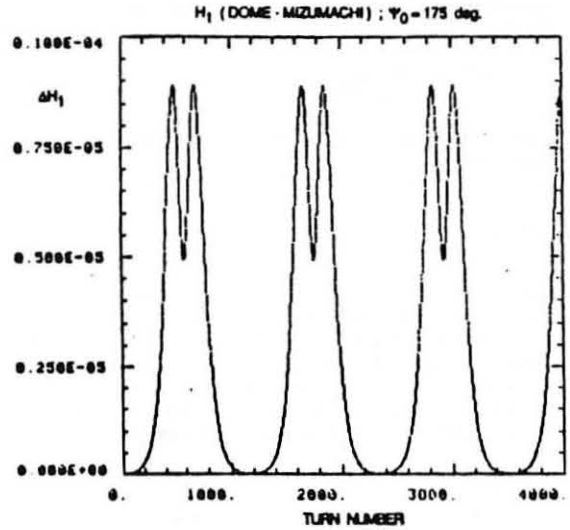

Fig. 2(a)

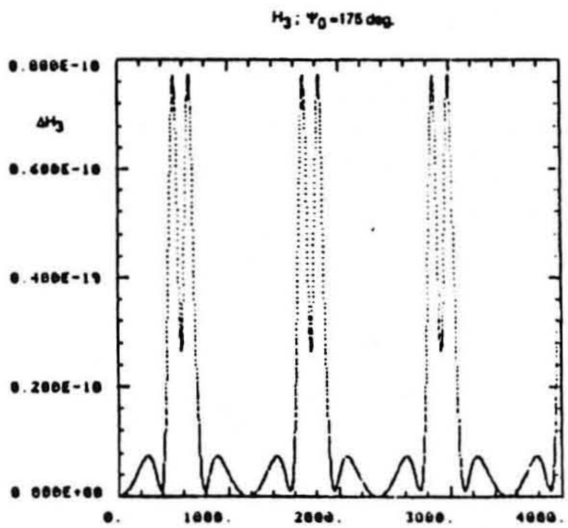

Fig. 2(b)

4. Generation of RF Noise for Synchrotron Phase-Space Tracking

The phase noise of the rf cavity voltage is characterized by a power spectrum and hence a certain autocorrelation in time (via a Fourier transformation). The noise seen by a particle turn-by-turn is correlated temporally according to this autocorrelation function. It is necessary for the tracking algorithm to be able to construct random phase noise at any turn, based on its value(s) at previous turn(s), such that the generated noise over a large number of turns is consistent with the known autocorrelation pattern. This is the classic problem of mean square estimation in noise theory.[7]

In the limiting case of a memory-less noise source corresponding to delta-correlation in time, the noise is trivially generated by sampling a certain (Gaussian, for example) distribution of random variables, generated by a random number generator with different seeds, keeping the rms σ of the distribution the same at all samplings.

For finite autocorrelation times, we have to include memory effects. For arbitrary correlation pattern with M-step memory, we estimate the noise φ_n at the n^{th} step by the linear combination of the past M values

$$\varphi_n^{es} = \sum_{m=1}^{M} a_m \varphi_{n-m} \ . \qquad (26)$$

Demanding that the error $(\varphi_n - \varphi_n^{es})$ be orthogonal to the data $(\varphi_{n-1}, \ldots, \varphi_{n-M})$ i.e.,

$$\langle \varphi_{n-1} - \sum_{m=1}^{M} a_m \varphi_{n-m} | \varphi_{n-p} \rangle = 0 \text{ for } p = 1, \ldots M \qquad (27)$$

guarantees that the mean square error $\langle |\varphi_n \ \varphi_n^{es}|^2 \rangle$ is minimum.[7] The coefficients a_m are then determined by solving the M simultaneous Eqs. (27) for the M unknowns a_m's in terms of the autocorrelations $R_m = \langle \varphi_n | \varphi_{n-m} \rangle$, for stationary noise. The conditional variance at the n^{th} step, given $\varphi_{n-1}, \ldots, \varphi_{n-M}$, equals the mean square estimation error[7]

$$\sigma^2_{\varphi_n | \varphi_{n-1}, \ldots, \varphi_{n-M}} = \langle |\varphi_n - \sum_{m=1}^{M} a_m \varphi_{n-m}|^2 \rangle$$

$$= R_0 - \sum_{m=1}^{M} a_m R_m \ . \qquad (28)$$

The generated noise sequence $\{\varphi_n\}$ is said to form a M-point Markov chain. The algorithm gets unnecessarily complicated for M>2. In the following we provide two algorithms for M = 1 and 2.

(a) One-point Markov chain algorithm

This is the usual Markov process where the noise at the n^{th} step depends on only the noise at the $(n-1)^{th}$ step. The noise generation follows a simple one-step hopping technique as illustrated in Fig. 3, according to the following linear mean square estimation procedure

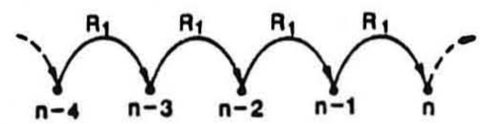

Fig. 3

$$\varphi_n^{es} = a_1 \varphi_{n-1} \qquad (29)$$

$$\langle \varphi_n - a_1 \varphi_{n-1} | \varphi_{n-1} \rangle = 0 \Rightarrow a_1 = R_1 / R_0 \qquad (30)$$

$$\sigma^2_{\varphi_n | \varphi_{n-1}} = R_0 - a_1 R_1 = \sigma_0^2 (1 - a_1^2) \quad (\sigma_0^2 = R_0) \ . \qquad (31)$$

Stationarity and Markovian character demands $R_n R_m = R_{n+m}$ which implies the unique solution $R_n = \sigma_0^2 e^{-\alpha n}$

the localized rf cavity (thin lens longitudinally), rather than relative to the jittery rf waveform with noise. In the frame of this absolute clock run by the ideal cavity, the synchrotron map with phase noise may be rewritten as

$$p_{n+1} - p_n = -kg(\psi_n + \varphi_n)$$

$$\psi_{n+1} - \psi_n = p_{n+1} \quad . \qquad (25)$$

This is the form we used in the actual tracking.

The phase noise φ_n results from the sampling of a random process every turn. For tracking with Eq. (25), one will have to generate sequences of these random numbers $\{\varphi_n\}$, consistent with the realistic noise characteristics of a driven rf cavity. We thus turn to this issue in the next section.

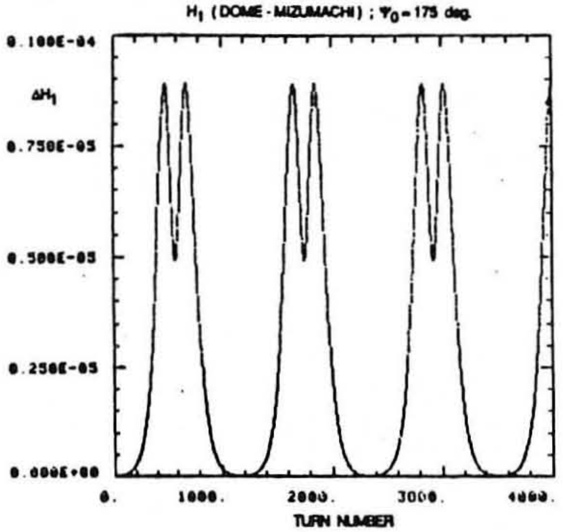

Fig. 2(a)

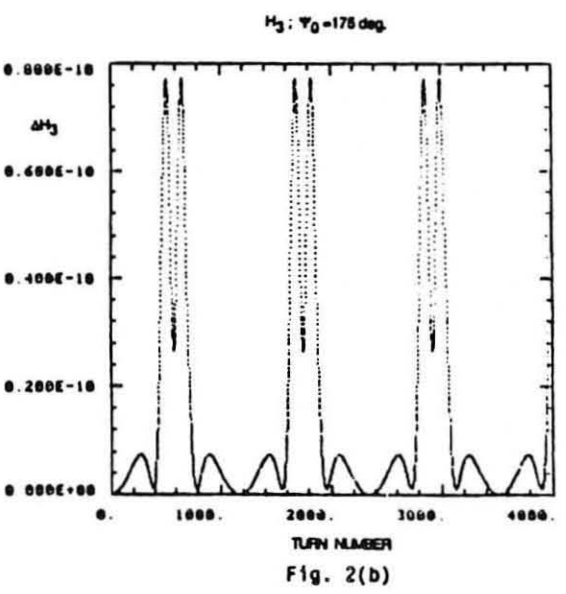

Fig. 2(b)

4. Generation of RF Noise for Synchrotron Phase-Space Tracking

The phase noise of the rf cavity voltage is characterized by a power spectrum and hence a certain autocorrelation in time (via a Fourier transformation). The noise seen by a particle turn-by-turn is correlated temporally according to this autocorrelation function. It is necessary for the tracking algorithm to be able to construct random phase noise at any turn, based on its value(s) at previous turn(s), such that the generated noise over a large number of turns is consistent with the known autocorrelation pattern. This is the classic problem of mean square estimation in noise theory.[7]

In the limiting case of a memory-less noise source corresponding to delta-correlation in time, the noise is trivially generated by sampling a certain (Gaussian, for example) distribution of random variables, generated by a random number generator with different seeds, keeping the rms σ of the distribution the same at all samplings.

For finite autocorrelation times, we have to include memory effects. For arbitrary correlation pattern with M-step memory, we estimate the noise φ_n at the n^{th} step by the linear combination of the past M values

$$\varphi_n^{es} = \sum_{m=1}^{M} a_m \varphi_{n-m} \quad . \qquad (26)$$

Demanding that the error $(\varphi_n - \varphi_n^{es})$ be orthogonal to the data $(\varphi_{n-1}, \dots, \varphi_{n-M})$ i.e.,

$$\langle \varphi_{n-1} - \sum_{m=1}^{M} a_m \varphi_{n-m} | \varphi_{n-p} \rangle = 0 \text{ for } p = 1,\dots M \qquad (27)$$

guarantees that the mean square error $\langle|\varphi_n \ \varphi_n^{es}|^2\rangle$ is minimum.[7] The coefficients a_m are then determined by solving the M simultaneous Eqs. (27) for the M unknowns a_m's in terms of the autocorrelations $R_m = \langle\varphi_n|\varphi_{n-m}\rangle$, for stationary noise. The conditional variance at the n^{th} step, given $\varphi_{n-1}, \dots, \varphi_{n-M}$, equals the mean square estimation error[7]

$$\sigma^2_{\varphi_n|\varphi_{n-1},\dots,\varphi_{n-M}} = \langle|\varphi_n - \sum_{m=1}^{M} a_m \varphi_{n-m}|^2\rangle$$

$$= R_0 - \sum_{m=1}^{M} a_m R_m \quad . \qquad (28)$$

The generated noise sequence $\{\varphi_n\}$ is said to form a M-point Markov chain. The algorithm gets unnecessarily complicated for M>2. In the following we provide two algorithms for M = 1 and 2.

(a) One-point Markov chain algorithm

This is the usual Markov process where the noise at the n^{th} step depends on only the noise at the $(n-1)^{th}$ step. The noise generation follows a simple one-step hopping technique as illustrated in Fig. 3, according to the following linear mean square estimation procedure

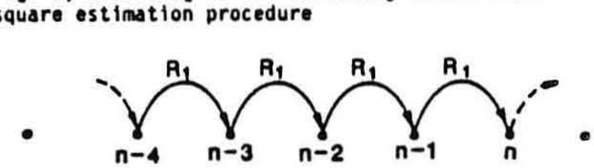

Fig. 3

$$\varphi_n^{es} = a_1 \varphi_{n-1} \qquad (29)$$

$$\langle\varphi_n - a_1\varphi_{n-1}|\varphi_{n-1}\rangle = 0 \Rightarrow a_1 = R_1/R_0 \qquad (30)$$

$$\sigma^2_{\varphi_n|\varphi_{n-1}} = R_0 - a_1 R_1 = \sigma_0^2(1-a_1^2) \ (\sigma_0^2 = R_0) \quad . \qquad (31)$$

Stationarity and Markovian character demands $R_n R_m = R_{n+m}$ which implies the unique solution $R_n = \sigma_0^2 e^{-\alpha n}$

the above expectation, as shown by the results plotted in Fig. 5. The growth of σ_I scales with the strength of noise σ_{noise} and the agreement of the above two stays preserved. The actual tracking included 2×10^3 revolutions in the ring.

The long term transport coefficients of diffusion

$$A_1 = \frac{\langle I_n - I_0 \rangle}{nT_r} \text{ and } A_2 = \frac{\langle (I_n - I_0)^2 \rangle}{nT_r} \tag{42}$$

(T_r = revolution time) can be derived from short term single particle tracking with independent noise samples for several synchrotron periods. The results have been compared to a direct numerical iteration of the Lie-algebraic map $\mathcal{M}(n)$ for the motion with noise [Eq. (24) or (25)] given by

$$\begin{aligned}
& I_n = \mathcal{M}(n)\, I_0 \\
& \mathcal{M}(n) = \exp(:-P_0 f_1:)\exp(:P_1 f_2:)\ldots\ldots \\
& \exp(:-P_{n-1} f_n:)\mathcal{M}_0^n \\
& f_n = \varphi_n - \varphi_{n-1} \\
& (I_n - I_o) = -\sum_{i=1}^{n+1} [\mathcal{M}_0^{i-1} P_0,\, I_0] f_i \\
& + \frac{1}{2} \sum_{i=1}^{n+1} \mathcal{M}_0^{i-1} [P_0, [P_0,\, I_0]] f_i^2 \\
& + \sum_{i=1}^{n+1} \sum_{j=i+1}^{n+1} [\mathcal{M}_0^{i-1} P_0, [\mathcal{M}_0^{j-1} P_0,\, I_0]]\, f_i f_j + \ldots
\end{aligned} \tag{43}$$

and then performing averages over noise samples. Here $\mathcal{M}_0$ is the map without noise. The agreement of the two results are exact within computer accuracy. Using Eq. (43), one can also verify analytically that the coefficients A_1 and A_2 in Eq. (42) satisfy the usual fluctuation-dissipation relation $A_1 = -\frac{1}{2}\partial A_2/\partial I_0$. This is consistent with the observed zero slope of Δ_I as a function of time (Fig. 7), since the slope of σ_I vs. time (Fig. 5,6) is found from tracking to be relatively independent of I_0 for the amplitudes considered.

The effect of the single step correlation (Eq. 29) on the growth rate of σ_I^2 for an ensemble of particles is shown in Figs. 6a and 6b. In this case an ensemble of 42 coherent particles, distributed along $H_s(\psi,P) = H_s(120 \text{ degrees}, 0)$ has been tracked for 200 synchrotron periods. Figure 6 shows the results for $\alpha = 0$ (zero turn-to-turn correlation), while the results for $\alpha = 0.5$ are shown in Fig. 6b. The observed effect is in agreement with the results obtained from averaging the square of the analytic equation (Eq. 43) for the appropriate noise model.

7. Conclusion

We have described some theoretical aspects of synchrotron phase-space tracking with rf phase-noise and feedback effects. Preliminary tracking results are consistent with expectations and validate the algorithm. The effects of phase feedback are presently under investigation.

References

1. D. Boussard and T.P.R. Linnecar, Proc. 12th Int. Conf. High Energy Accelerators, Fermilab, Aug. 11-16, 1983, pp. 226-228.
2. D. Boussard, Proc. CERN Accelerator School on Antiprotons for Colliding Beam Facilities, CERN-84-15, 1984, pp. 261-290.
3. G. Dome, ibid, pp. 215-260.
4. S. Krinsky and J.M. Wang, Part. Accelerators, 12, 107 (1982).
5. Y. Mizumachi, "Computer Simulation of Bunch Diffusion by rf Noise," SPS/AF/YM/ne/ 79-81, CERN, 1979.
6. E. Forest, B. Leemann, and S. Chattopadhyay, SSC-N-118, SSC Central Design Group Internal Report.
7. A. Papoulis, Probability, Random Variables and Stochastic Processes (McGraw-Hill, 1965).
8. S. Hansen et al., IEEE Trans. Nucl. Sci., Vol. NS-24, No. 3, June 1977.

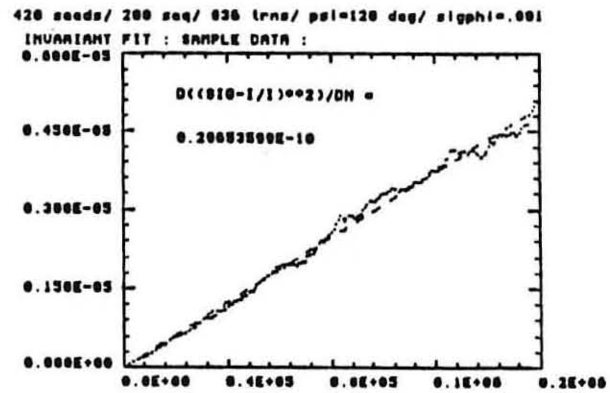

Fig. 5(a)

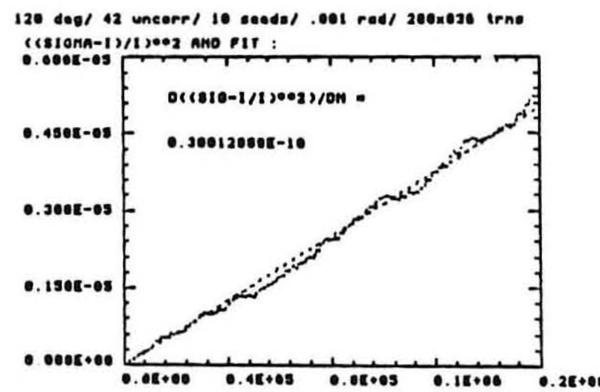

Fig. 5(b)

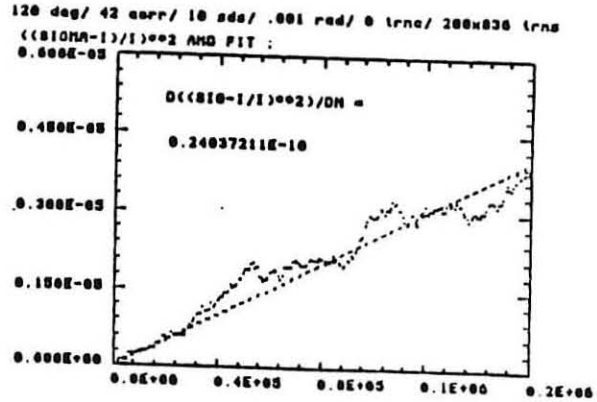

Fig. 6(a)

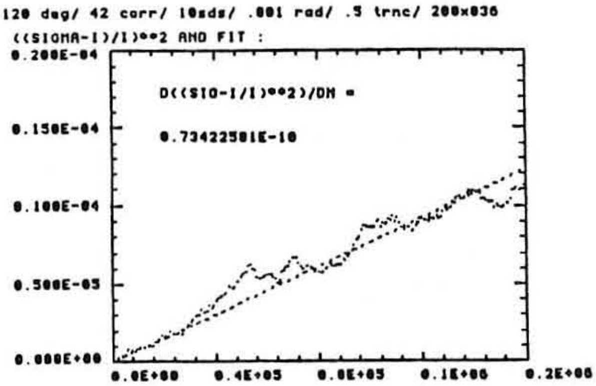
120 deg/ 42 corr/ 10sds/ .001 rad/ .5 trnc/ 200x036
((SIGMA-I)/I)**2 AND FIT :
D((SIG-I/I)**2)/DN =
0.73422501E-10
0.200E-04
0.150E-04
0.100E-04
0.500E-05
0.000E+00
0.0E+00
0.4E+05
0.8E+05
0.1E+06
0.2E+06

Fig. 6(b)

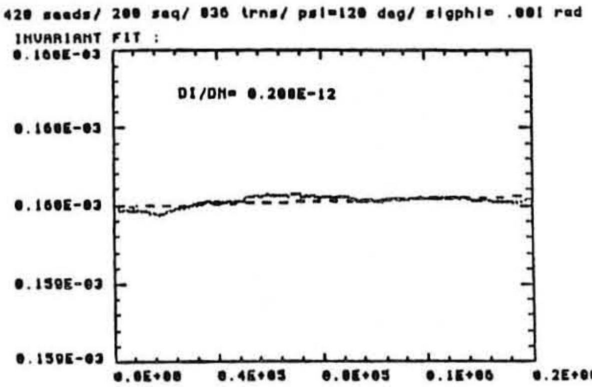
420 seeds/ 200 seq/ 036 trns/ psi=120 deg/ sigphi= .001 rad
INVARIANT FIT :
DI/DN= 0.200E-12
0.160E-03
0.160E-03
0.160E-03
0.159E-03
0.159E-03
0.0E+00
0.4E+05
0.8E+05
0.1E+06
0.2E+06

Fig. 7